RSC Advances

ROYAL SOCIETY OF CHEMISTRY

www.rsc.org/advances

Graphical abstract

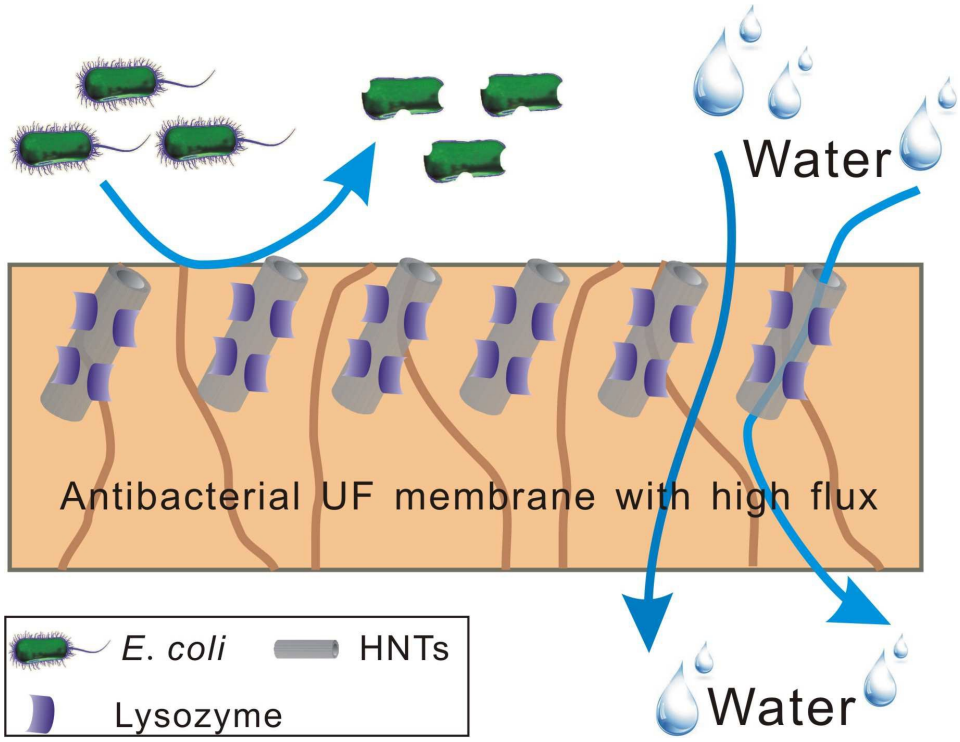

RSC Advances

RSC Publishing

Paper

Development of a novel polyethersulfone ultrafiltration membrane with antibacterial activity and high flux containing halloysite nanotubes loaded with lysozyme

Received
Accepted

www.rsc.org/

Qianqian Zhao [a], Chuochuo Liu [a], Jindun Liu [a], Yatao Zhang [a, b]*

In this study, halloysite nanotubes (HNTs) were used to immobilize lysozyme *via* covalent binding reaction. Immobilized lysozyme (HNTs-Ly) was then added into polyethersulfone (PES) polymer solution to prepare hybrid antibacterial ultrafiltration membranes *via* classic phase inversion. The results showed that the surface hydrophilicity and water flux of the hybrid membranes were significantly improved after adding HNTs-Ly. When the content of HNTs-Ly was 3.0 wt%, the water flux of resulted membranes could achieve to be as high as 400 $L \cdot m^{-2} \cdot h^{-1}$, and keep higher rejections for PEG 20000 (69%) and PVA 30000-70000 (99.6%). The tensile strength and elongation at break of the hybrid membranes reinforced after adding HNTs-Ly which revealed the mechanical strength of the membranes was also enhanced. Moreover, the hybrid membrane showed a good antibacterial property against Gram-negative bacteria (*E. coli*) with a high bacteriostasis rate of 63%.

Introduction

Ultrafiltration membranes, one of new unit operations in chemical engineering, have been playing momentous role in removal of low concentration pollutant in wastewater treatment, preparing ultra pure water, concentrating, separating and purifying medicine, and food processing because of low energy consumption and selective separation.[1-6] Polyethersulfone (PES) is always used to prepare ultrafiltration membranes on account of its excellent chemical, thermal stability, oxidation resistance and mechanical strength. [7, 8] Nevertheless, the inherent hydrophobic character of pure PES ultrafiltration membrane often leads to fouling during separation process, which reduces productivity, shortens membrane life, and changes membrane selectivity.[9] Plenty of studies have been devoted to improving the resistance ability of protein-fouling and biofouling of membranes. For protein-fouling, the commonly used approach is to reinforce the hydrophilicity and reduce the roughness of membrane surface.[10] Meanwhile, the associated efforts to decrease biofouling always include introduction of antibacterial groups to membrane matrix or utilization of antibacterial polymers used as membrane material.[11] Till now, various kinds of methods have been adopted to fabricate antibacterial membranes, such as coating,[12] surface grafting polymerization[13] and blending modification.[14] Because of easy operation, mild condition and neglectful influence for surface and cross-section structure of the membrane for blending modification, therefore, several antibacterial agents had been used to fabricate antibacterial hybrid membrane *via* this method, such as inorganic antibacterial agents (Ag, Cu and TiO_2 particles, etc.) have advantages of difficult volatility, extensive antibacterial effect and strong durative.[2, 15-18] However, the high-cost and slow response resulted that inorganic antibacterial agents during utilization limited their applications to some extent. Organic antibacterial agents (PHMG, PVP, etc.) were selected as alternative candidate owing to high bacteria-killing effects, which always exhibit bad chemical stability, drug-fast and thermostability.[7, 19] Compared with inorganic and organic antibacterial agents, natural antibacterial agents, like chitosan, chitin, enzyme, etc., have higher superiority for environment and human health.[20-22]

Enzyme, the biocatalyst, exists as high activity, selectivity, and specificity. Herein, Lysozyme belongs to the family of hydrolase for cell walls of microbe, making it a good candidate in antibacterial applications. Nevertheless, the reaction condition of enzymes is rigorous that permits chemical processes under the mildest experimental and environmental conditions, which needs many ways to improve enzyme features, as immobilization, if reasonably designed, it can improve almost all enzyme properties.[23] Moreover, direct addition of enzymes to membrane matrix is less efficient because of the loss of enzyme,[24] whereas immobilized enzymes could outstandingly enhance their stability.[25] Saeki et al.,[22] prepared polyamide reverse osmosis (RO) membrane through the covalent immobilization of enzymes, which decreased the water flux but maintained the salt rejection ratio, sufficient antibacterial activity against the *Gram-positive bacteria*, *Micrococcus lysodeikticus* and *Bacillus subtilis*. Wang et al.,[26] reported the successful immobilization of lipase enzyme in fibers *via* electrospinning of aqueous mixture of lipase and polyvinyl alcohol (PVA). It was conformed that the catalytic

activity of immobilized enzyme was the same as the crude enzyme.

Halloysite nanotubes (HNTs), a type of aluminosilicate clay, possess unique hollow and lathy tubular structure consisting of silicon-oxygen tetrahedron on the external surface and aluminum-oxygen octahedron on the internal surface. The superior physical-chemical properties of HNTs comprising of high length-diameter ratio and big specific surface area have attracted increasing attention in a wide field. [27, 28] Chen et al.,[29] synthesized halloysite nanotubes-chitosan-Ag nanoparticles (HNTs-CS@Ag) and then blended with PES to prepare antibacterial PES ultrafiltration hybrid membrane, which showed a good antibacterial activity against *Escherichia coli* and *Staphylococcus aureus*. HNTs also exhibited environmentally safe property. Fakhrullina et al., [30] have studied the toxicity of halloysite clay nanotubes *in vivo* employing *Caenorhabditis elegans* nematode and found that HNTs were not capable to severely damage the organism of the nematodes.

Herein, HNTs were functionalized with carboxylic groups (HNTs-COOH) and then lysozyme was covalently immobilized onto the surface of modified HNTs. Subsequently, a novel antibacterial PES ultrafiltration hybrid membrane was prepared *via* blending with HNTs-Ly through phase inversion method. These hybrid membranes were expected to display the treatment of water with good antibacterial properties.

Experimental

Materials

Polyethersulfone (PES, WM=58 kDa) was supplied by BASF Company, Germany. Halloysite nanotubes (HNTs) were refined from clay minerals in Henan province, China. 1, 6-hexamethylene diisocyanate (HMDI), dibutyltin dilaurate, lysozyme and fluorescein isothiocyanate were purchased from J&K. Butanedioic anhydride was purchased from Shanghai Chemical Reagent Research Institute. All the other chemicals (analytical grade) were obtained from Tianjin Kermel Chemical Reagent Co., Ltd., China and were used without further purification. The test strains, *E. coli* (8099) used for this study were provided by College of Public Health of Zhengzhou University. The used water is deionized water.

Synthesis of HNTs-Ly

The grafting of isocyano on HNTs (HNTs-NCO). The powders of HNTs were obtained by milling, sieving and then drying in a Muffle furnace at 573 K for 12 h. HNTs powders (2 g) were dispersed into acetone (60 g) with ultrasound for 1 h to form a suspension of HNTs. Thereafter, HMDI (1 g) was added in the above suspension and then dibutyltin dilaurate (0.1 g) was added to stir for 4 h at 70°C under reflux conditions at a nitrogen atmosphere. After cooling to room temperature, the obtained pink powder was collected by filtering, washing with acetone for several times and drying 50°C under vacuum for overnight.

The grafting of carboxyl on HNTs-NCO (HNTs-COOH). As-prepared HNTs-NCO (2 g) was dispersed in acetone (60 g) with ultrasound for 1 h, and then butanedioic anhydride (3 g), dibutyltin dilaurate (0.1 g) was added at a nitrogen atmosphere to react at 70°C for 3 h under constant stirring and reflux conditions. At last, the final precipitation was collected by filtration, washed with ethyl alcohol for 3 times, and dried in a vacuum oven at 50°C for 24 h.

The immobilization of lysozyme on HNTs-COOH. EDC (5 mg) and NHS (6 g) were added to 100 mL of phosphate buffer (0.2 M, pH=6.2), then, HNTs-COOH (0.3 mg) was dispersed into the aforementioned solution with the assistance of ultrasound at room temperature for 30 minutes. Lysozyme (120 mg) was added to HNTs-COOH suspension in phosphate buffer and shook continuously at 200 rpm for 24 h at 4°C. The precipitation was acquired by centrifugation, then washed with phosphate buffer for several times and vacuum freeze drying. The reaction principle of immobilizing lysozyme on HNTs is showed in Fig. 1.

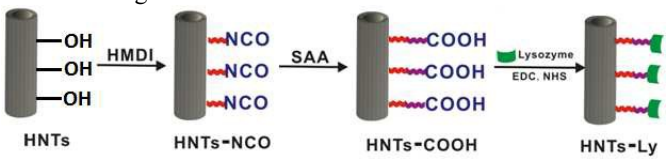

Fig. 1 Reaction principle of immobilizing lysozyme on HNTs

Fabrication of PES/HNTs-Ly antibacterial hybrid membrane

PES membrane and PES/HNTs-Ly antibacterial hybrid membrane were prepared by phase inversion method using casting solutions including PES (18 wt%), polyvinylpyrrolidone (PVP) (at 8 wt% constant concentration) as pore former, bits of acetone, different concentrations of HNTs-Ly powder (1 wt%, 2 wt%, and 3 wt% by weight of PES) in N,N-dimethylacetamide (DMAc) (73.2 wt%) as solvent. For preparing the homogonous casting solution, firstly, a certain amount of HNTs-Ly was dispersed into DMAc with ultrasonic treatment, subsequently, PES, acetone and PVP were added to HNTs-Ly suspension under stirring by mechanical stirrer at room temperature for 15 h to fabricate transparent and homogonous casting solution which was filtered and degassed under vacuum at room temperature for at least 4 h without stirring. Finally, the above solution was cast onto a clean glass plate by self-made casting knife with 0.1 mm thickness and then immersed in coagulation bath (deionized water, 40°C) for precipitation. After complete precipitation, the membranes were kept in deionized water at ambient temperature for at least 24 h to complete phase separation and remove the remaining solvent prior to further characterization.

Characterization of HNTs

Fourier transforms infrared spectroscopy (FTIR). The chemical composition of raw HNTs and modified HNTs (HNTS-NCO, HNTs-COOH, and HNTs-Ly) were all characterized using FT-IR Thermo Nicolet IR 200 spectroscope (Thermo Nicolet Corporation, USA). Typically, 64 scans were signal-averaged to reduce spectral noise. The spectra were recorded in the 400-4000 cm^{-1} range using KBr pellets.

Thermo-gravimetric analysis (TGA). TGA measurements were performed on a TG-DTA, DT-40 system (Shimadzu, Japan). For this purpose, ca. 3 mg samples were filled into an alumina crucible and heated from room temperature to 800°C at 10°C per min under flowing nitrogen.

Transmission electron microscopy (TEM). The morphology of HNTs and modified HNTs were investigated by a FEI model TECNAI G^2 transmission electron microscope (200 kV acceleration voltages). The samples for analysis were dispersed in ethanol with the aid of ultrasound and then the suspended particles were transferred to and allowed to dry on a copper grid (400 meshes) coated with a strong carbon film.

Fluorescent microscopic analysis. Lysozyme was labeled with fluorescein isothiocyanate (FITC-Ly) and then the labeled samples were used for the immobilization process. The immobilization and distribution of lysozyme on the surface of HNTs were examined by a BM-21AY fluorescence microscope (Shanghai BM optical instrument manufacturing Co., Ltd, China) with the fluorescence excitation wavelength of 450-490 nm.

Characterization of membranes

Water contact angle. The water contact angle of the membranes was measured on a contact angle goniometer (OCA20, Dataphysics Instruments, and Germany) at 25°C and 50% relative humidity. 1 μL of deionized water was carefully dropped on the top surface and the contact angle between the water and membrane was measured until no further change was observed. To minimize the experimental error, the contact angle was measured at five random locations for each sample and then the average was reported.

Scanning electron microscopy (SEM). A scanning electron microscope (JSM-6700F, JEOL, and Japan) was used for the morphology observation of the membrane cross-section and plane. Samples of the membranes were frozen in liquid nitrogen and then fractured. The membranes were sputtered with gold, which were viewed with the microscope at 10 kV.

Mechanical properties. Tensile strength and percentage elongation were measured on testing strips using a model UTM2203 electronic universal testing machine (Jinan Huike Test Instrument Co., Ltd., China) mounted with a 100 N load cell at room temperature at a constant crosshead speed of 5 mm/min with aluminum sample holder. The membranes were cut into 40 mm × 10 mm pieces and the thickness of the membranes was obtained from the SEM results of membranes. Particular attention was given to the macroscopic homogeneity of membranes and only apparently homogeneous membranes were used for the mechanical tests.

Separation performance of membranes. The separation performance of the prepared membranes was measured by a cross-flow filtration system. The effective area of each flat sheet membrane pieces is 22.2 cm^2. Each membrane was compacted at 0.2 MPa for 1 h prior to performing the ultrafiltration experiments. Then the pressure was lowered to 0.1 MPa and all the ultrafiltration experiments were carried out at this pressure. After compacted, the pure water flux was recorded at ambient temperature. The PEG 20000 solution (0.5 g/L) and PVA 30000-70000 solution (0.5 g/L) were forced to permeate through the membrane and the permeate solutions were collected. The permeation flux (J) and rejection (R) were calculated using the following equation:

$$J = \frac{V}{A \times T} \qquad (1)$$

Where V is the volume of permeate pure water (L), A is the effective area of the membrane (m^2), and T is the permeation time (h).

$$R = \left(1 - \frac{C_P}{C_f}\right) \times 100\% \qquad (2)$$

Where C_p is the permeate concentration and C_f is the feed concentration (mg/L). The concentrations of PEG 20000 and PVA 30000–70000 were obtained by a UV–vis spectrophotometer (Shimadzu, Japan). The detailed procedure for PEG or PVP determination was given elsewhere. [9]

Antibacterial activity tests. Minimal inhibitory concentration (MIC) tests were performed to study the quantitative antibacterial properties of HNTs-Ly. A quantity of *E. coli* cells suspended solution (10^6 CFU /mL) was prepared to reserve. Antibacterial agents (ca. 0.6826 mg) were dissolved in 1 mL of Luria-Bertani (LB) liquid nutrient medium with the concentration of 512 μg/mL. Subsequently, *E. coli* cells suspended solution (1 mL) was added in the solution with different content of antibacterial agents (512, 256, 128, 64, 32 μg/mL), respectively. Containing only 2 mL of the bacterium solution and only 2 mL of LB were regarded as control groups. Then, the seven samples were shaken for 2 h at 37°C. After that, bacterium solution was diluted with sterile water till its concentration becomes 10^{-4} of the cultured, 0.2 mL of dilution solution was uniform coating on plates and incubated at 37°C for 12 h. The numbers of colonies on the plates were determined by the plate count method. The bacteriostasis rate (B_R) was calculated using the following equation.

$$B_R = \frac{A - B}{A} \times 100\% \qquad (3)$$

Where A is the number of bacterial colonies on the plates from the control group and B is the number of bacterial colonies on the plates from the experiment group.

Moreover, bacteriostasis rate was also used in order to quantitatively analyze the antibacterial activity of the membranes. A quantity of *E. coli* cells suspended solution (10^6 CFU /mL) was prepared to reserve. All the membrane samples (ca. 0.06 g) were cut and sterilized by autoclaving for 20 min, respectively. To test the antibacterial activity, the membranes were added into the 5 mL solution incubated by about 10^6 cells/mL of the *E. coli* bacterium solution, and then incubated at 37°C for 4 h with shaking. After that, membranes were retrieved from cultures and washed by normal saline. The wash solutions were collected and diluted it with deionized water till its concentration becomes 10^{-5} of the original value. 0.1 mL of dilution solution was spread onto LB culture medium and all plates were incubated at 37°C for 24 h. The numbers of colonies on the plates were determined by the plate count method and bacteriostasis rate (B_R) was defined by the above equation (3).

Long time water flux performance of membranes. A long time (48 h, per 30 min) water flux performance of membrane was also measured by the cross-flow filtration system with pure water. The effective area of each flat sheet membrane pieces is 22.2 cm^2. The pressure was set at 0.1 MPa and all the tests are carried out at this pressure. After compaction, the pure water flux was recorded at ambient temperature every 30 minutes. Flux drop (ΔJ) was calculated by using the following equation:

$$\Delta J = \left(1 - \frac{J_x}{J_1}\right) \times 100\% \qquad (4)$$

Where J_1 is the water flux for 30 min, J_x is the water flux for 30x min (x=1, 2, ...96).

Results and discussion

Characterization of HNTs-Ly

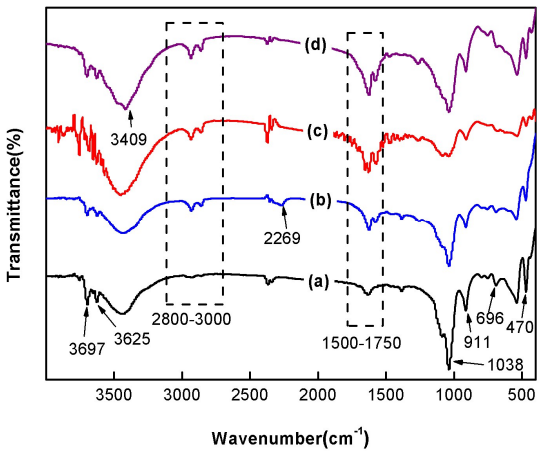

Fig. 2 FT-IR spectra of (a) raw HNTs, (b) HNTs-NCO, (c) HNTs-COOH and (d) HNTs-Ly

The chemical structures of the unmodified and modified HNTs were characterized by FTIR. Fig. 2 shows the FTIR spectra of raw HNTs, HNTs-NCO, HNTs-COOH and HNTs-Ly. Compared with Fig. 2(a) (the raw HNTs), the spectra around 2933 cm^{-1} and 2852 cm^{-1} are ascribed to the C-H stretching vibration in CH_2 and CH_3. The peaks around 2269 cm^{-1} are assigned to -NCO asymmetric stretching vibration and the absorption peak at 1579 cm^{-1} is the stretch vibration of the -NHCO- bonds in the HNTs-NCO. From Fig. 2(c), the C=O stretching vibrations in the carboxyl group of N-COOH are obviously visible around 1750 cm^{-1}, whereas the peaks around 2269 cm^{-1} disappear, which declared that -NCO was turned into -COOH. From Fig. 2(d), the CH_2 absorption peaks at 2933 cm^{-1} and 2852 cm^{-1} are stronger, which because the density methyl and methylene are reinforced after the immobilization of lysozyme. The above results confirmed that lysozyme was immobilized on the HNTs.

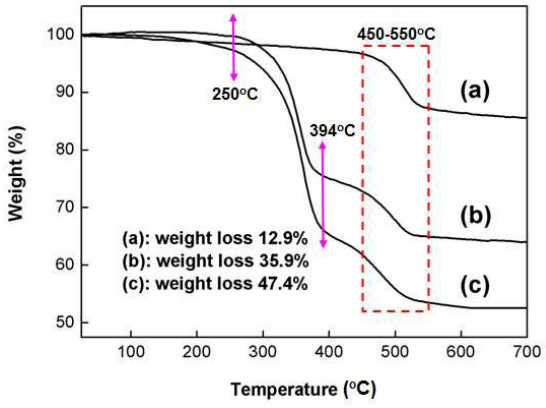

Fig. 3 TGA curves of (a) raw HNTs, (b) HNTs-NCO, and (c) HNTs-COOH

In order to further confirm the modification of HNTs, Fig. 3 displays the TGA curves of (a) raw HNTs, (b) HNTs-NCO and (c) HNTs-COOH. For the curve of raw HNTs, an obvious mass loss was resolved in the range of 450-550°C. This mass loss was assigned to the dehydroxylation of structural Al-OH groups of HNTs.[31] The first mass loss in the range 50-150°C was due to physically adsorbed water.[32] For curves of (b) and (c), both curves showed distinct mass loss which can be attributed to decomposition of the HMDI and SAA of modified HNTs, which also demonstrated that -COOH groups were grafted onto the HNTs successfully. From the TGA analysis, the content of -NCO and -COOH could be obtained and are about 0.3 g (-NCO) per g (HNTs) and 0.13 g (-COOH) per g (HNTs-NCO), respectively.

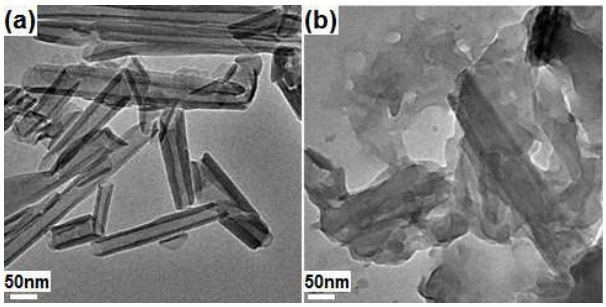

Fig. 4 TEM images of (a) raw HNTs and (b) HNTs-Ly

Fig. 4 displays TEM images of HNTs (a) and HNTs-Ly (b). As shown in Fig. 4(a), the morphology of raw HNTs apparently exhibit hollow tubular and open-ended structure. From Fig. 4(b), the surface of HNTs is adhered irregular viscous precipitations which have big particle size. Therefore, the results demonstrated that lysozyme was successfully immobilized on the surface of HNTs-COOH.

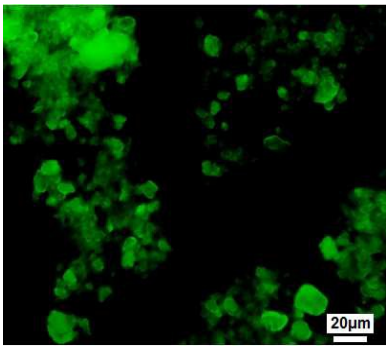

Fig. 5 Fluorescence microscopic image of HNTs-Ly

Fluorescence microscopic image of HNTs-Ly is shown in Fig. 5. FITC-Ly was immobilized on the HNTs-COOH through the covalent bond, immobilized enzymes presented bright yellow-green fluorescence under fluorescence microscope with 490 nm of excitation wavelength. This result demonstrated that lysozyme was successfully immobilized on the surface of HNTs-COOH.

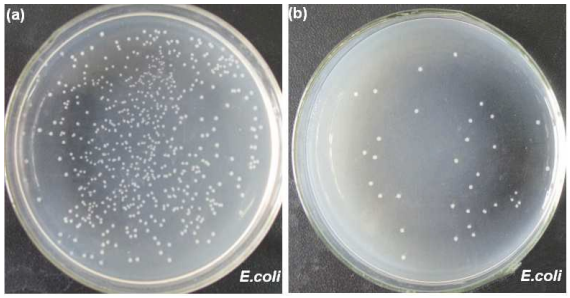

Fig. 6 Antibacterial effect of (a) control and (b) HNTs-Ly against *E.coli*

The antibacterial effect is shown in Fig. 6. Compared with the control (see Fig. 6(a)), Fig. 6(b) shows that HNTs-Ly particles

exhibit a significant antibacterial property with less *E. coli* colonies. Therefore, the results indicated that HNTs-Ly had antibacterial efficacy for *E. coli*. The MIC and the bacteriostasis rate of HNTs-Ly were 512 μg/mL and 94.9%, respectively.

Characterization of PES/HNTs-Ly hybrid membranes

Morphology of membranes.

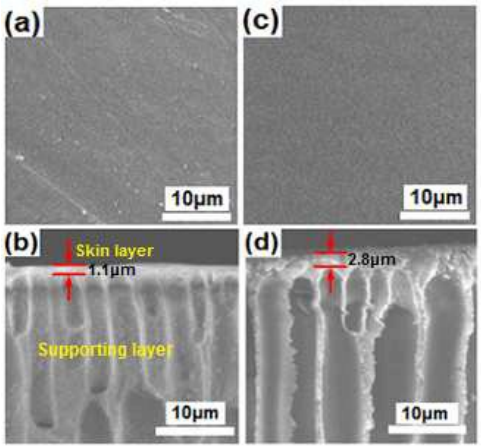

Fig. 7 SEM images of the surface morphology of (a) PES membrane, (c) PES/HNTs-Ly hybrid membrane and the cross-section of (b) PES membrane, (d) PES/HNTs-Ly hybrid membrane

Fig. 7 displays the SEM images of (a, b) pure PES membranes and (c, d) hybrid membrane with HNTs-Ly loading amount of 3 wt%. As can be seen in the SEM images (a) and (c), the surface of PES/HNTs-Ly hybrid membrane became much smoother compared with pure PES membrane. It is generally recognized that membrane with smooth surface has higher antifouling and hydrophilicity behavior compared to that with rough surface.[33] Fig. 7(b, d) show the cross-section morphologies of the tested membranes. Both PES membrane and hybrid membrane have dense skin layer and finger-like structural support layer. However, it can be observed a significant increase in macrovoids pore size of support layer, like the scale of Fig. 7(b, d), which would enhance the permeation flux of the membrane. The enlarged pore size of macrovoids may result from the increase in thermodynamic instability of the cast film, which promotes a rapid phase separation.[34]

Hydrophilicity of membranes.

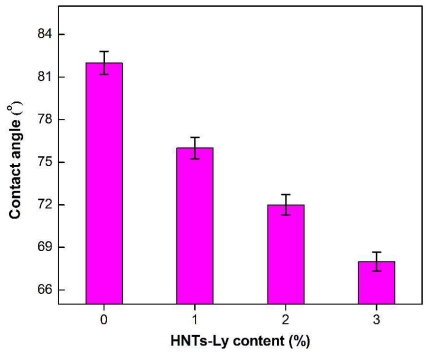

Fig. 8 Effect of HNTs-Ly content on water contact angle of PES/HNTs-Ly hybrid membranes

Surface hydrophilicity is one of the most important factors for ultrafiltration membranes in determining antifouling property. However, PES is an intrinsically hydrophobic polymer; thereby hydrophilic modification is indispensable for PES ultrafiltration membranes. In this study, water contact angle measurement was selected to evaluate the relative hydrophilicity or hydrophobicity of membrane surface and provide information on the interaction energy between the surface and liquid.[7] It is generally accepted that the lower contact angle represents the greater tendency for water to wet the membrane, the higher surface energy and the higher hydrophilicity.[9] From Fig. 8 it can be found that the pure PES membrane presents the highest contact angle of 82° and this value decreased with the increase of the HNTs-Ly, which indicated that the hybrid membrane exhibited superior hydrophilicity on account of the introduction of HNTs-Ly. During the formation process of hybrid membranes, HNTs-Ly in the casting solution tend to migrate spontaneously to the surface of the hybrid membranes to reduce the interface energy[34] which lead to an increase in membrane hydrophilicity. As shown in Fig. 8, the lowest contact angle decreased to 67° when the adding amount of HNTs-Ly reached 3 wt%. The results proved that the accretion of HNTs-Ly could reinforce the hydrophilicity of PES membranes.

Permeation property of membranes.

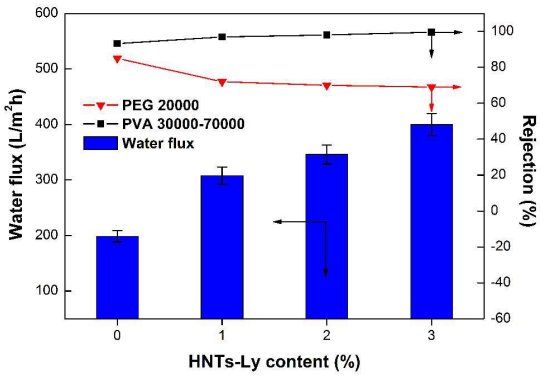

Fig. 9 Effect of HNTs-Ly content on separation performance of PES/HNTs-Ly hybrid membranes

Pure water flux and the rejections for PEG 20000 and PVA 30000–70000 of the hybrid membranes with different HNTs-Ly contents (1 wt%, 2 wt%, 3 wt%) are illustrated in Fig. 9. Pure water flux increased quickly after adding HNTs-Ly. When the content of HNTs-Ly is 3 wt%, the pure water flux reached to be the maximum of 400 $L \cdot m^{-2} \cdot h^{-1}$ compared with 198.5 $L \cdot m^{-2} \cdot h^{-1}$ of pure PES membranes. The phenomenon is consistent with the results of contact angle. Meanwhile, the rejection for PVA 30000–70000 could keep above 99.6%. These results might be explained as follows: Physical sieving by pores is believed to be the main driving factor in the ultrafiltration membrane. The diameter of water molecular was smaller than the pores size on the skin layer of PES membrane, so it could be premitted through the membrane under the pressure difference. However, the water flux of pure PES membrane was lower than PES/HNTs-Ly membrane because of the inherent hydrophobic character of PES, and the enhanced pure water flux also might be attributed to the addition of hydrophilic HNTs-Ly and the hollow structure of HNTs which may facilitate water transmission. The principle of increasing water flux for the hybrid membranes was described in Fig. 10. Those performances are consistent with the latest researches.[9, 35]

Moreover, the big particle size of HNTs-Ly may result in more interface voids around HNTs-Ly particles thereby producing additional pathways for water molecules. However, a slight increase in PVA 30000–70000 rejection may result from the thickened skin layer (as observed in Fig. 7) which provide more steric resistance for PVA molecules. Such higher rejection for PVA 30000-70000 was quite similar to our previous work.[36] While the rejection of the membranes against PEG 20000 decreased slightly by the additions of HNTs-Ly due to its smaller molar mass compared with PVA 30000-70000.

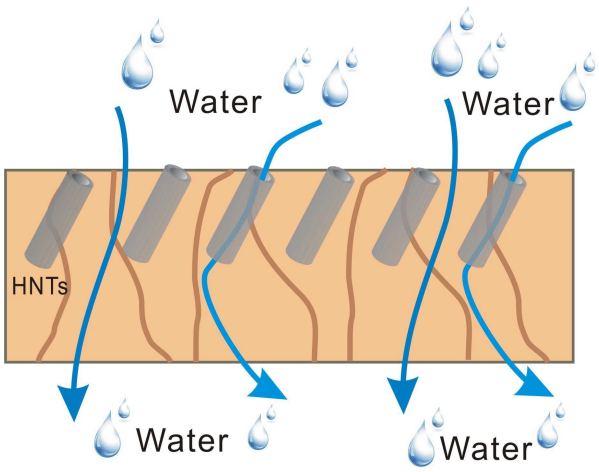

Fig. 10 Principle of increasing water flux for PES/HNTs-Ly hybrid membranes

Mechanical properties of membranes.

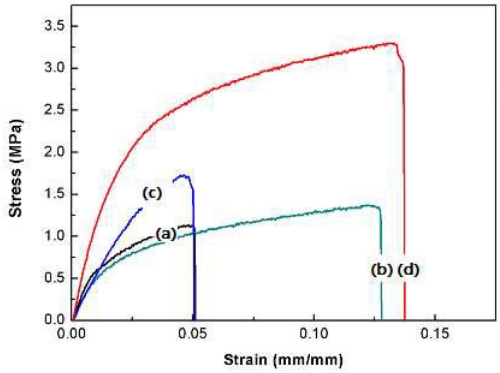

Fig. 11 Stress-strain curves of (a) PES membrane, (b-d) PES/HNTs-Ly membranes with different HNTs-Ly content (1 wt%, 2 wt%, 3 wt%, respectively)

Fig. 11 shows the stress-strain curves of the test membranes obtained from the mechanical measurements. From Fig. 11, tensile strength increased from 1.13 MPa to 3.30 MPa with increasing HNTs-Ly content from 0 wt% to 3 wt%. The phenomenon is consistent with the widespread theory that organic-inorganic hybrid membranes combine the flexibility of organic membrane and stiffness of inorganic membrane. However, elongation at break changed erratically, which might be caused by agglomerations and voids of immobilized lysozyme in membranes and the decrease in homogeneity of hybrid membrane. When the content of HNTs-Ly adds up to 3 wt%, both of them achieve to maximize. Briefly, the mechanical properties of membranes are mainly affected by the cross-linking of additive molecules and the homogeneity of membranes. Thus, the above results indicated that the incorporation of HNTs-Ly could observably improve mechanical stabilities of PES membranes, making them useful for some higher pressure conditions.

Antibacterial performance of membranes.

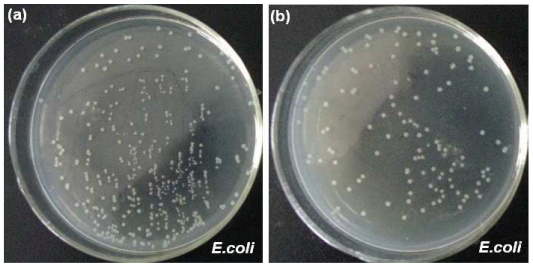

Fig. 12 Antibacterial effect of (a) PES membrane and (b) PES/HNTs-Ly hybrid membranes with 3 wt% of HNTs-Ly against *E.coli*

Table 1 Antibacterial rate of the PES/HNTs-Ly hybrid membranes against *E. coli*

	E. coli	
	Bacterial colonies (cfu)	Antibacterial rate (%)
Pure PES membrane	314	-
Hybrid membranes with 3 wt% HNTs-Ly	116	63

The antibacterial effect is reflected in Fig. 12 and the bacteriostasis rate is presented in Table 1. Compared with pure PES membrane, it is clear seen that the number of colonies on the plates treated with hybrid membranes containing 3 wt% HNTs-Ly decreased significantly. The bacteriostasis rates of the hybrid membranes against *E. coli* were 63%, which indicated the excellent inhibiting effect of immobilized lysozyme for *E. coli*, because it is generally deemed that the higher bacteriostasis rate demonstrates the better antibacterial ability. On the other hand, it was also certified that immobilized lysozyme was intercalated into the PES membranes. Simultaneously, Fig. 13 clearly exhibited the antibacterial mechanism of the membranes with HNTs-Ly. The above results suggested that PES/HNTs-Ly membranes had a preferable antibacterial ability which mainly attributed to the introduction of HNTs-Ly.

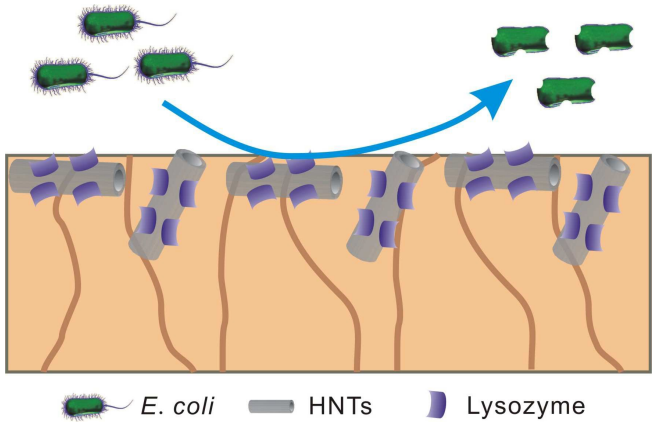

Fig. 13 Antibacterial mechanism of the PES/HNTs-Ly hybrid membranes

Long time water flux performance of membranes.

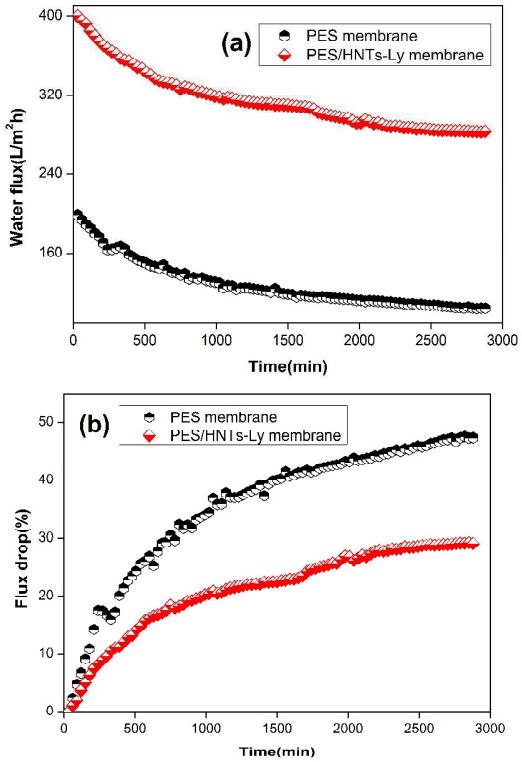

Fig. 14 (a) Water flux and (b) flux drop of PES and PES/HNTs-Ly hybrid membranes in long time run

A long time (48 h) water flux test of PES membrane and PES/HNTs-Ly membrane with 3 wt% HNTs-Ly is shown in Fig. 14 (a). It can be seen that the water flux of membranes is decreasing with respect to time, which may be caused by blocking of the pores of membranes. Fig. 14 (b) illustrates the flux drop of membranes. Interestingly, the flux drop of PES/HNTs-Ly membrane is smaller than PES membrane, obviously. It indicates that the addition of hydrophilic HNTs-Ly has efficaciously restrained the pollutant adhered to the membrane surface and improved the antifouling property of PES membranes.

Conclusions

In summary, a novel antibacterial particle, HNTs-Ly was successfully prepared *via* covalently immobilized lysozyme onto the surface of modified HNTs. Subsequently, PES/HNTs-Ly hybrid ultrafiltration membranes were fabricated by classical phase inversion method. The hydrophilicity and mechanical properties of the hybrid membranes increased significantly compared with the pure PES membranes. In addition, the antibacterial properties of the hybrid membranes were also improved. Therefore, these membranes exhibit the potential to reduce the fouling in water treatment.

Acknowledgements

This work was financially sponsored by the National Natural Science Foundation of China (Nos. 21376225 and 21106137), and China Postdoctoral Science Foundation (Nos. 2014T70686 and 2013M531684). We sincerely acknowledge the financial assistance of visiting research program in University of New South Wales by the China Scholarship Council (No. 201208410135).

Notes and references

[a] *School of Chemical Engineering and Energy, Zhengzhou University, Zhengzhou 450001, China*
E-mail: zhangyatao@zzu.edu.cn
[b] *UNESCO Centre for Membrane Science and Technology, School of Chemical Engineering, University of New South Wales, Sydney, NSW 2052, Australia*

1. M. A. Barakat, *Arab. J. Chem.*, 2011, **4**, 361.
2. J.-n. Shen, H.-m. Ruan, L.-g. Wu and C.-j. Gao, *Chem. Eng. J.*, 2011, **168**, 1272.
3. A. Idris, N. Mat Zain and M. Y. Noordin, *Desalination*, 2007, **207**, 324.
4. W. Guo, H. H. Ngo and J. Li, *Bioresour. Technol.*, 2012, **122**, 27.
5. M. A. Shannon, P. W. Bohn, M. Elimelech, J. G. Georgiadis, B. J. Marinas and A. M. Mayes, *Nature*, 2008, **452**, 301.
6. D. Rana and T. Matsuura, *Chem. Rev.*, 2010, **110**, 2448.
7. W. Zhao, J. Huang, B. Fang, S. Nie, N. Yi, B. Su, H. Li and C. Zhao, *J. Membr. Sci.*, 2011, **369**, 258.
8. J. C. Dang, Y. T. Zhang, Z. Du, H. Q. Zhang and J. D. Liu, *Water Sci. Technol.*, 2012, **66**, 799.
9. L. Yu, Y. Zhang, B. Zhang, J. Liu, H. Zhang and C. Song, *J. Membr. Sci.*, 2013, **447**, 452.
10. S. Boributh, A. Chanachai and R. Jiraratananon, *J. Membr. Sci.*, 2009, **342**, 97.
11. J. Mansouri, S. Harrisson and V. Chen, *J. Mater. Chem.*, 2010, **20**, 4567.
12. C. Wang, F. Yang and H. Zhang, *Sep. Purif. Technol.*, 2010, **75**, 358.
13. B. Fang, Q. Ling, W. Zhao, Y. Ma, P. Bai, Q. Wei, H. Li and C. Zhao, *J. Membr. Sci.*, 2009, **329**, 46.
14. H. Basri, A. F. Ismail and M. Aziz, *Desalination*, 2011, **273**, 72.
15. Y. Chen, Y. Zhang, J. Liu, H. Zhang and K. Wang, *Chem. Eng. J.*, 2012, **210**, 298.
16. Y. Liu, X. Wang, F. Yang and X. Yang, *Micropor. Mesopor. Mater.*, 2008, **114**, 431.
17. X. Zhang, T. Zhang, J. Ng and D. D. Sun, *Adv. Fun. Mater.*, 2009, **19**, 3731.
18. Y. F. Chen, J. C. Dang, Y. T. Zhang, H. Q. Zhang and J. D. Liu, *Water Sci. Technol.*, 2013, **67**, 1519.
19. J. Nikkola, X. Liu, Y. Li, M. Raulio, H.-L. Alakomi, J. Wei and C. Y. Tang, *J. Membr. Sci.*, 2013, **444**, 192.
20. S. Chen, G. Wu, D. Long and Y. Liu, *Carbohydr. Polym.*, 2006, **64**, 92.
21. J. Yao, R. Chen, K. Wang and H. Wang, *Micropor. Mesopor. Mater.*, 2013, **165**, 200.
22. D. Saeki, S. Nagao, I. Sawada, Y. Ohmukai, T. Maruyama and H. Matsuyama, *J. Membr. Sci.*, 2013, **428**, 403.
23. C. Mateo, J. M. Palomo, G. Fernandez-Lorente, J. M. Guisan and R. Fernandez-Lafuente, *Enzyme Microb. Tech.*, 2007, **40**, 1451.
24. F. N. Crespilho, M. Emilia Ghica, M. Florescu, F. C. Nart, O. N. Oliveira and C. M. A. Brett, *Electrochem. Commune.*, 2006, **8**, 1665.
25. D. N. Tran and K. J. Balkus, *ACS Catal.*, 2011, **1**, 956.
26. Y. Wang and Y. L. Hsieh, *J. Membr. Sci.*, 2008, **309**, 73.
27. Y. Lvov and E. Abdullayev, *Prog. Polym. Sci.*, 2013, **38**, 1690.
28. Y. Zhang, Y. Chen, H. Zhang, B. Zhang and J. Liu, *J. Inorg. Biochem.*, 2013, **118**, 59.
29. Y. Chen, Y. Zhang, H. Zhang, J. Liu and C. Song, *Chem. Eng. J.*, 2013, **228**, 12.
30. G. I. Fakhrullina, F. S. Akhatova, Y. M. Lvov and R. F. Fakhrullin, *Environ. Sci.: Nano,* 2015, **2**, 54.
31. S. Barrientos-Ramírez, G. M. d. Oca-Ramírez, E. V. Ramos-Fernández, A. Sepúlveda-Escribano, M. M. Pastor-Blas and A. González-Montiel, *Applied Catalysis A: General*, 2011, **406**, 22.
32. S. Barrientos-Ramírez, E. V. Ramos-Fernández, J. Silvestre-Albero, A. Sepúlveda-Escribano, M. M. Pastor-Blas and A. González-Montiel, *Micropor. Mesopor. Mater.*, 2009, **120**, 132.

33. J. Y. Zhang, Y. T. Zhang, Y. F. Chen, L. Du, B. Zhang, H. Q. Zhang, J. D. Liu and K. J. Wang, *Ind. Eng. Chem. Res.*, 2012, **51**, 3081.
34. V. Vatanpour, S. S. Madaeni, L. Rajabi, S. Zinadini and A. A. Derakhshan, *J. Membr. Sci.*, 2012, **401-402**, 132.
35. J. Zhu, N. Guo, Y. Zhang, L. Yu and J. Liu, *J. Membr. Sci.*, 2014, **465**, 91.
36. H. Yu, Y. Zhang, J. Zhang, H. Zhang and J. Liu, *Des. Water Treat.*, 2013, **51**, 3584.

